doi.org/10.36721/PJPS/2026.40.16912.1

Metabolomic profiling and quantitative comparison of inflorescences and succulent stems of *Cynomorium songaricum* Rupr. to evaluate their chemical resource potential

Congying Li[1,2], Zhongjie Bai[2], Qin Wang[2], Yuxia Song[2], Jiaqi Hu[2], Lin Yang[3] and Yumei Wang[2]*

[1]Key Laboratory of Hexi Corridor Resources Utilization, Gansu Province, Zhangye 734000, China
[2]Hexi University, Zhangye 734000, China
[3]Maternal and Child Health Institute in Ganzhou District, Zhangye 734000, China

Abstract: **Background**: *Cynomorium songaricum* Rupr. is a national Class-II protected, kidney-yang-tonifying medicinal herb. According to pharmacopoeia standards, only succulent stems are used medicinally, whereas inflorescences are discarded during processing, leading to massive resource waste. Previous studies have lacked systematic, multi-platform chemical comparisons of these two tissues, hindering rational reuse of inflorescence by-products. **Objectives**: This study aimed to characterize chemical differences between inflorescences and succulent stems through targeted quantification and broad-spectrum metabolomics to evaluate the potential of discarded inflorescence by-products as chemical resources for sustainable resource utilization. **Methods**: UV–visible spectrophotometry and high-performance liquid chromatography quantified total flavonoids, polysaccharides and three phenolic markers. Targeted ultra-performance liquid chromatography-tandem mass spectrometry metabolomics combined with principal component analysis and orthogonal partial least squares discriminant analysis was performed to screen differential metabolites. **Results**: Succulent stems contained higher total flavonoids (140.30 vs. 69.27 mg·g^{-1}), gallic acid (4.5475 mg·g^{-1}, undetected in inflorescences), *p*-hydroxybenzoic acid (0.2935 vs. 0.1220 mg·g^{-1}) and catechin (8.7567 vs. 1.4385 mg·g^{-1}). Inflorescences contained more total polysaccharides (279.87 vs. 224.26 mg·g^{-1}). In total, 469 differential metabolites were annotated. Specifically, 351 metabolites (mainly flavonoids and amino-acid derivatives) were enriched in succulent stems; 118 metabolites (lignans, coumarins and terpenoids) accumulated in inflorescences. **Conclusion**: Discarded inflorescences possess abundant tissue-specific bioactive constituents, indicating potential for resource exploitation based on chemical profiles alone. This work provides chemical evidence supporting the reutilization of inflorescences, which may help mitigate overharvesting pressure on wild succulent stems and support circular conservation of this endangered medicinal plant. Such resource potential is inferred from metabolite profiling rather than from proven pharmacological efficacy. Further pharmacological validation of kidney-yang-tonifying activity and safety assessment are required before any medicinal application.

Keywords: Bioactive components; *Cynomorium songaricum* Rupr.; Inflorescences; Metabolomics; Succulent stems

Submitted 05-06-2026 – Revised 30-08-2026 – Accepted 10-09-2026

Article in Press

INTRODUCTION

Cynomorium songaricum Rupr. (*C. songaricum*), a precious parasitic medicinal herb that mainly parasitizes *Nitraria* L. (Zygophyllaceae) (Zhang *et al*., 2022b), has been widely used in traditional medicine to tonify kidney-yang, replenish essence and moisten the intestines to alleviate constipation (Qin *et al*., 2025). Driven by expanding market demand, rampant wild harvesting has drastically diminished its natural population; therefore, this species has been classified as a national protected Class II wild plant (Wang *et al*., 2023). Wild harvesting of *C. songaricum* imposes multiple sustainability risks. Collecting whole wild plants removes the underground succulent stems together with the haustorial connection to their *Nitraria* host, which often kills the entire parasite and may damage host root systems. Unregulated large-scale collection reduces natural recruitment and hinders wild population regeneration. The Chinese Pharmacopoeia (2025 Edition) defines its sole official medicinal material with explicit processing requirements: 'This product is the dried succulent stems of *C. songaricum* collected by digging whole plants in spring, removing inflorescences, cutting them into sections and drying them.' Governed by this statutory standard, all clinical formulations, commercial herbal processing workflows and most published phytochemical investigations exclusively studied succulent stems, while inflorescences stripped during raw material sorting are fully discarded without medicinal utilization as there are no established medicinal utilization pathways (Aruna *et al*., 2025; Zhang *et al*., 2023). The simultaneous pressures of dwindling wild stocks and complete wastage of inflorescence biomass exacerbate resource depletion, thus highlighting an urgent need to systematically compare the chemical profiles of inflorescences and succulent stems.

**Corresponding author:* e-mail: lcyvsxp@163.com

Collectively, previous phytochemical and metabolomic studies of *C. songaricum* have three unresolved research gaps that limit its rational and sustainable resource exploitation. First, almost all published research exclusively targets the pharmacopoeia-specified succulent stems (Zhang *et al*., 2025; Aruna *et al*., 2025); only a small number of flavonoid monomers have been superficially isolated from discarded inflorescences, without simultaneous quantitative comparison or full-spectrum metabolomic profiling between the two tissues (Zhang *et al*., 2007; Ma and Chen, 2008). No study has systematically clarified tissue-specific accumulation patterns of major bioactive compounds in inflorescences, leaving the chemical basis of its medicinal value uncharacterized. Second, conventional quality evaluation systems rely on single or dual chemical markers and lack an integrated, multi-index quantitative framework to distinguish tissue chemical differences comprehensively (Meng *et al*., 2023; Wang *et al*., 2024). Third, existing analytical work relies on isolated detection techniques (UV–visible spectrophotometry [UV–vis], high-performance liquid chromatography [HPLC], or single metabolomic detection alone) rather than a multi-layered combined analytical workflow, thus failing to construct a holistic chemical evidence chain to interpret metabolic divergence between inflorescences and succulent stems (Song *et al*., 2025; Meng *et al*., 2023). Based on the traditional medicinal record, existing phytochemical reports and industrial waste status of *C. songaricum*, a testable core hypothesis was proposed to guide all analytical workflows and subsequent data interpretation: the discarded inflorescences of *C. songaricum* contain abundant tissue-specific metabolites with distinct chemical profiles compared with succulent stems and hence may merit further exploration for resource-development value, rather than representing chemically inert waste material. Analogous to other high-value applications of agro-forestry processing by-products, discarded plant fractions are not necessarily chemically inert waste. Comprehensive chemical profiling is a critical prerequisite for evaluating their resource-exploitation potential before industrial development (Feng *et al*., 2026). To fill the three critical gaps and verify the proposed hypothesis, the present study was conducted to develop three targeted methodological systems: first, a multi-index quantitative platform integrating UV–vis and validated HPLC to synchronously detect multiple indicator compounds, overcome the defects of single-marker quality assessment and reveal tissue-specific distribution patterns of targeted components; second, widely targeted ultra performance liquid chromatography-tandem mass spectrometry (UPLC-MS/MS) metabolomics to perform full-spectrum metabolic profiling of two tissue types, annotate tissue-differentiated phytochemicals and identify differential accumulation patterns invisible to single-component quantification; third, an integrated multi-platform analytical pipeline combining macro-component spectrophotometric detection, targeted HPLC phenolic quantification and metabolomic fingerprinting to comprehensively characterize inter-tissue chemical discrepancies and provide chemical evidence for evaluating the reutilization prospect of waste inflorescence biomass.

Polysaccharides and flavonoids are the primary bioactive substances of *C. songaricum* (Lan *et al*., 2025; Qin *et al*., 2025), while gallic acid, *p*-hydroxybenzoic acid and catechin are core phenolic quality markers closely associated with its pharmacological efficacy (Zhang *et al*., 2021; Guo *et al*., 2022). These five components were selected as joint evaluation indicators in this study, with three rationales as follows. First, gallic acid and catechin have been validated as reliable chromatographic markers to differentiate *C. songaricum* samples from different origins, processing technologies and tissue parts and *p*-hydroxybenzoic acid is stably detectable in both inflorescences and succulent stems and shares homologous phenolic skeletons with the other two phenolic markers (Guo *et al*., 2022; Zhang *et al*., 2021). Second, the five target compounds all have well-documented antioxidant, anti-fatigue, neuroprotective and anti-inflammatory activities, which closely match the traditional therapeutic effects of *C. songaricum*, including tonifying kidney-yang, slowing aging and relaxing bowels (Lyu *et al*., 2023; Ma *et al*., 2023; Yu *et al*., 2008). Third, these analytes show ideal analytical performance for routine HPLC quantification, with wide linear ranges, low limits of detection/quantitation and stable extraction recoveries (Meng *et al*., 2023). Accordingly, systematic comparative quantification of polysaccharides, flavonoids and three phenolic markers between succulent stems and inflorescences is essential to verify whether inflorescences are valueless processing waste, unravel tissue-specific metabolic differentiation and lay a chemical foundation for developing inflorescences as complementary medicinal resources.

Widely targeted metabolomics stands out for its high throughput, superior sensitivity and accurate metabolite annotation and has become a mainstream tool for comparing tissue-wide metabolic fingerprints in medicinal plants (Liu *et al*., 2025). Advancements in liquid chromatography-mass spectrometry (LC-MS)-based analytical workflows, including UPLC-Q-TOF-MS combined with molecular networking and widely targeted UPLC-MS/MS strategies, have greatly facilitated large-scale metabolite characterization of complex herbal extracts, thus enabling efficient screening and structural elucidation of diverse secondary metabolites from traditional Chinese medicines (Peng *et al*., 2024; Wu *et al*., 2024a). Such multi-platform LC-MS strategies can resolve complex chemical matrices, discriminate tissue-specific metabolite distribution patterns and uncover bioactive constituents hidden in different plant organs. Leveraging LC-MS, the overall research strategy of the present work is

Article in Press

as follows: UV–vis, targeted HPLC quantification and broad-spectrum UPLC-MS/MS metabolomics were combined to conduct the first comprehensive chemical comparison of inflorescences and succulent stems of *C. songaricum*. This multi-dimensional analytical strategy can overcome the limitations of single-technique detection, systematically characterize the differential accumulation of flavonoids, polysaccharides, phenolic compounds and other phytochemical classes across the two tissues and provide complementary experimental evidence to support the recycling of discarded inflorescence biomass. Ultimately, the information from this study is expected to help ease overharvesting pressure on wild succulent stems, enable the circular utilization of protected *C. songaricum* resources and fill the research gap on the chemical basis of inflorescence by-products. This work also followed the concept of conservation-oriented phytochemistry, which advocates comprehensive chemical profiling of processing by-products before industrial exploitation of endangered medicinal herbs (Shi *et al*., 2022).

MATERIALS AND METHODS

Plant materials and chemicals

Whole plants of *C. songaricum* were purchased in April 2024 from Damo Agriculture and Forestry Ecological Industry Co., Ltd. (Jiuquan City, China). All individuals were cultivated in uniform desert saline-alkali soil and were uniformly parasitized by *Nitraria* L., with consistent cultivation duration and field management to eliminate geographical and habitat-induced metabolic differences. Fifty intact, morphologically uniform whole plants were purchased as the original experimental materials. All plant specimens were authenticated as the whole herb of *C. songaricum* by Associate Professor Congying Li, School of Medicine, Hexi University. The voucher specimen (batch no. CS-20240410) was deposited in the Herbarium of Key Laboratory of Hexi Corridor Resources Utilization, Gansu Province for permanent traceability.

Reference standards, including gallic acid, *p*-hydroxybenzoic acid, catechin, rutin and glucose (purity ≥ 98%), were sourced from Shanghai Yuanye BioTechnology Co., Ltd. and Shandong Yousoo Chemical Co., Ltd. All other reagents and chromatographic solvents met analytical standards.

Sample preparation

Of the 50 purchased whole plants, 10 individual plants were preliminarily screened using unified criteria, including complete morphological integrity, consistent individual size, uniform growth status and the absence of disease or mechanical damage. Each plant was manually separated into inflorescence and succulent stem tissues. All tissue fragments were dried in an electro-thermostatic blast drying oven (Model DHG-9140A, Shanghai Qixin Scientific Instrument Co., Ltd.) at 45 °C, pulverized, passed through a 60-mesh sieve and then hermetically stored away from light. For quantitative analysis using a UV-2600 (220 V, CH, Shimadzu, Japan) UV-vis spectrophotometer and an LC-20AD (Shimadzu, Japan) HPLC system, all ten biological batches (each batch = one independent plant) of both tissue types were tested, with three independent technical replicates per biological batch to reduce manual error. For targeted UPLC-MS/MS (ExionLC™ AD, AB SCIEX) metabolomic profiling, three representative individual plants covering low, medium and high concentration gradients of total flavonoids and total polysaccharides were further screened as biological replicates for metabolomics analysis, based on the pre-determined total flavonoid and total polysaccharide quantitative data from the ten batches above.

Determination of total flavonoid and total polysaccharide contents

Sample preparation

Exactly 20.67 mg of rutin reference standard was weighed and transferred into a 100 mL volumetric flask. Subsequently, 50 mL of methanol was added to the flask and the mixture was heated using an HH-2 digital constant-temperature water bath (Changzhou Guohua Electric Appliance Co., Ltd.) to fully dissolve the solid. After cooling to ambient temperature, 50 mL of water was added and the solution was diluted to the mark and mixed thoroughly, yielding a stock solution containing 0.2067 $mg \cdot mL^{-1}$ rutin.

A total of 1.0057 g of glucose standard was accurately weighed, dissolved in ultrapure water in a 100 mL volumetric flask and diluted to the mark. Serial dilutions were performed twice (10 mL into 100 mL each time) to prepare a working standard solution with a final concentration of 100.57 $\mu g \cdot mL^{-1}$ glucose.

Next, add 50 mL of 60% aqueous ethanol to 1.0 g of pulverized inflorescence or succulent stem powder of *C. songaricum* in a 100 mL conical flask. The total mass of the flask and mixture was recorded before ultrasonic extraction for 30 min at 350 W and 50 °C using a KQ-500E numerical-control ultrasonic cleaner (Kunshan Ultrasonic Instruments Co., Ltd.). After cooling to 25 °C, the lost solvent weight was replenished with 60% aqueous ethanol. The mixture was vortexed and filtered and the subsequent filtrate was collected as the test solution for total flavonoid quantification.

Additionally, 0.5 g of each powdered tissue sample was accurately weighed into a 250 mL stoppered conical flask and extracted with 100 mL of 80% aqueous ethanol under reflux for 1 h to remove lipid and monosaccharide impurities. The hot mixture was filtered and the filter residue and filter were rinsed three times with 30 mL of hot 80% ethanol. All filter residues were quantitatively transferred into a new 250 mL stoppered flask with 150 mL

Article in Press

ultrapure water, then subjected to a second reflux extraction for 2 h. After cooling, the aqueous extract was transferred to a 200 mL volumetric flask and diluted to the mark with water. An aliquot of 5 mL filtrate was precisely transferred into a 25 mL volumetric flask and diluted with water to obtain 25 mL of test solution for total polysaccharide evaluation.

Detection methods

The aluminum nitrate-sodium nitrite colorimetric method was used to evaluate total flavonoids and absorbance was measured at 510 nm. To quantify total polysaccharides, the phenol-sulfuric acid method was used and absorbance was measured at 490 nm (Song *et al*., 2025).

Calibration curve construction

Graded volumes (0.5, 1, 2, 4, 6, 8, 10 mL) of the rutin stock solution prepared in *Sample preparation* (Determination of total flavonoid and total polysaccharide contents) were accurately transferred into separate 25 mL volumetric flasks and ultrapure water was added to 10 mL per flask. Then, 1 mL of 5% (w/v) sodium nitrite solution was added to each flask, mixed and incubated for 6 min. Next, 1 mL of 10% (w/v) aluminium nitrate solution was added; after mixing and another 6 min of incubation, 10 mL of 4% (w/v) sodium hydroxide solution was added. Each mixture was diluted to the mark with water, homogenized and equilibrated for 15 min. A blank control was prepared using the same procedure without rutin standard. The absorbance of each standard solution was recorded at 510 nm using a UV–vis spectrophotometer. A calibration curve was plotted with rutin concentration ($\mu g \cdot mL^{-1}$) on the x-axis and absorbance (A) on the y-axis.

Graded volumes (0.2, 0.4, 0.8, 1.2, 1.6, 2.0 mL) of the glucose working solution prepared as described under *Sample preparation* (Determination of total flavonoid and total polysaccharide contents) were pipetted into individual test tubes and water was added to adjust the total volume to 2.0 mL for each tube. After adding 1 mL of 5% (w/v) phenol solution to the tube and mixing thoroughly, 5 mL of concentrated sulfuric acid was rapidly incorporated, followed by manual vortex-mixing and 10 min of static incubation. The tubes were incubated in a 40 °C water bath for 15 min and immediately cooled to ambient temperature. A blank control was processed in parallel without glucose standard. Absorbance values were measured at 490 nm using UV–vis and the calibration curve was generated using glucose concentration ($\mu g \cdot mL^{-1}$) as the abscissa and absorbance (A) as the ordinate.

Methodological validation of UV–vis assay

Four core validation indicators were evaluated according to the guidelines of the Chinese Pharmacopoeia (2025 Edition) (National Pharmacopoeia Committee, 2025), with a unified qualification criterion of relative standard deviation (RSD) < 3.0%. (1) *Precision*: Single aliquots of the rutin and glucose standard working solutions were subjected to six consecutive absorbance measurements and the RSD was calculated. (2) *Repeatability*: Six parallel portions of the same tissue powder were weighed, extracted and tested independently, following which content RSD of the six parallel samples was calculated. (3) *Stability*: A single sample test solution was prepared and stored at room temperature, followed by absorbance measurement at 0, 2, 4, 8, 12, 24 h; solution stability was assessed via RSD. (4) *Recovery*: Nine portions of tissue powder with known flavonoid/polysaccharide content were weighed and divided into three groups (n=3 each). The standard substance was added to the groups at 80%, 100% and 120% of the intrinsic content, respectively, extracted and detected by following the full protocol. Recovery rate = (detected total content − intrinsic content)/spiked standard amount ×100%; acceptable recovery range: 95%–105%.

HPLC analysis of gallic acid, p-hydroxybenzoic acid and catechin

Sample preparation

Mixed reference solutions containing gallic acid, *p*-hydroxybenzoic acid and catechin at concentrations of 0.5340, 1.793 and 6.166 $mg \cdot mL^{-1}$, respectively, were prepared. Approximately 4.0 g of succulent stem powder was weighed, loaded into an extraction container and thoroughly homogenized with 50 mL methanol. Sonication extraction was performed at 55 °C with 350 W for 45 min and the sample was then allowed to cool to 30 °C prior to filtration. The filtrate was concentrated to 5 mL by rotary evaporation under reduced pressure and then passed through a 0.45 μm microporous filter membrane. The final filtrate was retained as the testing solution.

Chromatographic conditions

A Shimadzu InertSustain C18 column (250 mm × 4.6 mm, 5 μm) served as the separation medium. Methanol and 0.08% aqueous phosphoric acid were chosen as the two mobile phase components in the following gradient elution program: Methanol varied from 5% to 15% over 0–15 min, remained 15% from 15–50 min, climbed to 20% over 50–65 min, stayed at 20% from 65–85 min, rose to 65% from 85–105 min, remained 65% from 105–115 min, then dropped to 5% in the last 5 min. The analysis was carried out at a flow rate of 1.0 $mL \cdot min^{-1}$, column temperature of 35 °C, detection wavelength of 280 nm and sample injection volume of 10 μL.

HPLC calibration curve

First, 10 μL of each mixed gradient standard solution was injected into the HPLC system under the chromatographic conditions described in ***Chromatographic conditions*** and the peak area of each target compound was recorded. Standard mass concentration (x, $\mu g \cdot mL^{-1}$) was used as the horizontal coordinate, while the chromatographic peak area (y) was used as the vertical coordinate to perform

Article in Press

linear regression and generate linear equations and R^2 values.

Validation of analytical performance

All validation experiments complied with the 2025 Chinese Pharmacopoeia HPLC validation requirements, with criteria of RSD < 2.0% and a recovery range of 96%–105%. (1) *Precision*: The mixed standard solution containing three reference compounds was injected six times consecutively and the RSD of the peak areas was calculated. (2) *Repeatability*: Six parallel weighed powder samples were extracted and detected independently, followed by calculation of the content RSD of target phenolics. (3) *Sample solution stability*: The test solution was injected at 0, 4, 8, 10, 12 and 24 h and their peak area RSDs were compared. (4) *Recovery*: Six portions of tissue powder with known intrinsic content were divided into low, medium and high spike groups (n=3). Reference standards were added to each group at 80%, 100% and 120% endogenous content, respectively and fully extracted and quantified. Recovery rate was calculated using the same formula used for UV−Vis assay.

Determination of gallic acid, p-hydroxybenzoic acid and catechin

Ten batches containing inflorescence and succulent stem tissues of *C. songaricum* were collected. The three target compounds were assayed individually for each batch, with three parallel determinations per sample.

Widely targeted metabolomics analysis

Sample preparation

Extraction workflow: 50 mg pulverized tissue was mixed with 1200 μL ice-cold 70% methanol solution. The mixture was vortexed six times (30 s each), then centrifuged at 12,000 rpm for 3 min using an Eppendorf 5424R centrifuge. The resulting supernatant was filtered through a 0.22 μm microporous filter. Each of the three biological replicates of inflorescence and succulent stem powder was extracted independently following the above protocol. Six tissue extracts (3 batches × 2 tissue types) were obtained for metabolomic detection and each sample was injected once for UPLC-MS/MS acquisition without technical replicates. Quality control (QC) pooled samples were prepared by mixing equal volumes of all six sample extracts.

Chromatographic conditions

An Agilent SB-C18 column (2.1 mm × 100 mm, 1.8 μm) served as the stationary phase for compound separation. The analysis was performed at a column temperature of 40 °C and a flow rate of 0.35 mL·min^{-1}, with an injection volume of 2 μL. Two elution solvents were adopted for the mobile phase: 0.1% formic acid in water (A) and 0.1% formic acid in acetonitrile (B). The following gradient elution program was implemented: A decreased from 95% to 5% over 0–9 min, remained at 5% from 9–10 min, increased to 95% from 10–11 min and remained at 95% from 11–14 min.

Mass spectrometric conditions

The electrospray ionization (ESI) ion source temperature was adjusted to 550 °C. The ion spray (IS) voltages were fixed at 5500 V and −4500 V for the positive and negative ionization modes, respectively. The pressure of source gas I (GSI) was configured as 50 psi, source gas II (GS II) as 60 psi and curtain gas (CUR) as 25 psi, while the collision activation energy level was adjusted to high grade. Multiple reaction monitoring (MRM) scanning mode was adopted for data collection on the triple quadrupole mass spectrometer and nitrogen was used as the collision gas at medium intensity. Declustering potential (DP) and collision energy (CE) values were individually tuned to optimal levels. Based on the retention window of each eluting metabolite, distinct MRM ion transition groups were tracked in each acquisition time segment using the refined DP and CE parameters (Li *et al*., 2026).

Metabolite identification

Metabolite qualitative identification and relative quantification were performed by wide-target UPLC-MS/MS in MRM mode. Spectra were annotated using the proprietary MetWare database (MWDB, Wuhan Metware Biotechnology Co., Ltd.) via the intelligent MS/MS matching algorithm self-developed by the company. Four orthogonal descriptors were integrated for multidimensional metabolite matching: precursor-ion exact mass (acquired from full-scan MS), MS/MS fragment ions, isotopic distribution and chromatographic retention time (RT). Before spectral alignment, isotope noise, sodium/potassium cation adduct peaks and nonspecific background fragments were filtered to eliminate interference. Standardized matching tolerances were set at 20 ppm for precursor-ion mass deviations (from full-scan MS), 20 ppm for fragment-ion mass deviations (from MS/MS spectra) and 0.2 min for the RT drift between sample peaks and library reference spectra. The algorithm aligned sample fragmentation profiles, isotopic signatures and RT values pairwise against MWDB standard spectra to generate a unified composite matching score for each metabolite feature, which was then used to categorize all annotated compounds into three confidence tiers per MetWare's proprietary grading standards. Notably, no authentic chemical reference standards were independently injected to cross-validate any annotated metabolites in this widely targeted metabolomics workflow. Relative metabolite quantification was achieved using MRM peak areas acquired on a triple quadrupole mass spectrometer.

Statistical analysis

Quantitative results of total flavonoid, total polysaccharide and targeted phenolic compound content were presented as mean ± standard deviation (SD), derived from ten paired plant batches. Paired-samples Student's t-test was

Article in Press

conducted for content comparison between tissues in GraphPad Prism 11 Pro. The built-in report effect sizes function was activated to simultaneously generate t-values, p-values, 95% confidence intervals (95% CIs) of mean differences and Cohen's d effect sizes. The significance threshold was defined as $p < 0.05$.

For metabolomic datasets, the raw metabolomic data were processed in SIMCA software for multivariate statistical analysis; principal component analysis (PCA) and orthogonal partial least squares-discriminant analysis (OPLS-DA) were used to reveal distinct metabolic signatures between inflorescences and succulent stems of *C. songaricum*. To prevent model overfitting, the OPLS-DA model was verified using 200 permutation tests.
Univariate statistical analysis was performed simultaneously in R software to calculate Student's t-test p-values for each metabolite across two tissue groups. Benjamini–Hochberg (BH) false discovery rate (FDR) correction was applied to adjust raw p-values for multiple-testing bias, eliminating false-positive signals induced by simultaneous testing of hundreds of metabolite features. Differential metabolites were screened using three core complementary parameters to strictly reduce false discovery risk: (1) variable importance in the projection (VIP) scores from validated OPLS-DA model, VIP > 1; (2) fold change (FC), FC ≥ 2 or FC ≤ 0.5; (3) FDR-adjusted *p*-value < 0.05. Compounds meeting all three thresholds were defined as reliable differential metabolites for subsequent enrichment analysis. The KEGG pathway database was further used for functional annotation and pathway enrichment analysis of these FDR-filtered differential metabolites.

RESULTS

Determination of total flavonoids and total polysaccharides

Full methodological validation was performed for the UV–vis colorimetric assay. Rutin and glucose achieved favorable linearity (R^2 = 0.9999). All RSD values for repeatability, stability and precision were below 3.00%. The average recoveries were 97.32% for rutin and 102.53% for glucose, with RSD values of 2.90% and 2.88%, respectively. These results confirm the credibility and reproducibility of total flavonoid and polysaccharide contents for inter-tissue comparison. Tables S1 and S2 summarize all linearity, precision, stability and recovery validation data for the two colorimetric assays.

The total flavonoid content in succulent stems (140.2991 ± 34.1103 mg·g^{-1}) was approximately 2.0-fold higher than that in inflorescences (69.2710 ± 14.6580 mg·g^{-1}). The paired-samples t-test revealed a highly significant difference between the two tissues ($P < 0.001$). In contrast, the total polysaccharide content was significantly higher in inflorescences (279.8742 ± 46.4970 mg·g^{-1}) than in succulent stems (224.2648 ± 37.2970 mg·g^{-1}), with a highly significant inter-tissue difference ($P < 0.001$) (Table S3).

Quantitative levels of gallic acid, p-hydroxybenzoic acid and catechin

Under the established chromatographic conditions, HPLC chromatograms of inflorescences, succulent stems and the mixed reference standard were obtained. As shown in figure 1, all target peaks exhibited symmetrical peak shapes and satisfactory resolution, indicating excellent chromatographic separation. Tables S4 and S5 summarize all HPLC method validation data, including linearity, precision, stability and recovery. All RSD values were less than 2% and average recoveries fell within 96%–105%, which sufficiently supported the reliability of the quantitative data for the phenolic compounds between the two tissues.

The contents of these three components in the succulent stems and inflorescences were then determined; the results are presented in Table S6. Gallic acid had an average content of 4.5475 mg·g^{-1} in the succulent stems and was not detected in the inflorescences. The limit of detection (LOD) of gallic acid was 0.0320 μg·mL^{-1} (Table S4) and no distinguishable chromatographic peak matching the RT of gallic acid standard (Peak 1) was observed in the HPLC chromatogram of inflorescences (Fig. 1C), confirming the absence of quantifiable gallic acid in inflorescences. The content of *p*-hydroxybenzoic acid in succulent stems (0.2935 ± 0.1004 mg·g^{-1}) was approximately 2.4-fold that in inflorescences (0.1220 ± 0.0335 mg·g^{-1}) and the difference was highly significant ($P < 0.001$). Similarly, catechin content was markedly higher in succulent stems (8.7567 ± 3.9497 mg·g^{-1}) than in inflorescences (1.4385 ± 0.3262 mg·g^{-1}), with a highly significant difference ($P < 0.001$).

Metabolomic profiling and differential metabolites

To guarantee the precision, reproducibility and stability of metabolomic outputs, QC specimens were measured separately before, throughout and after the entire UPLC-MS/MS acquisition workflow. A total of six test samples (3 biological replicates each for inflorescences and succulent stems) alongside repeated pooled QC samples were continuously analysed within a single UPLC-MS/MS acquisition run. Total ion current (TIC) traces of QC extracts collected at distinct acquisition intervals under both positive and negative ionization scanning modes were superimposed and visualized in figure 2. The highly overlapping TIC profiles showed consistent retention times and ion signal intensities across all QC injections, confirming stable instrument performance throughout detection.

Article in Press

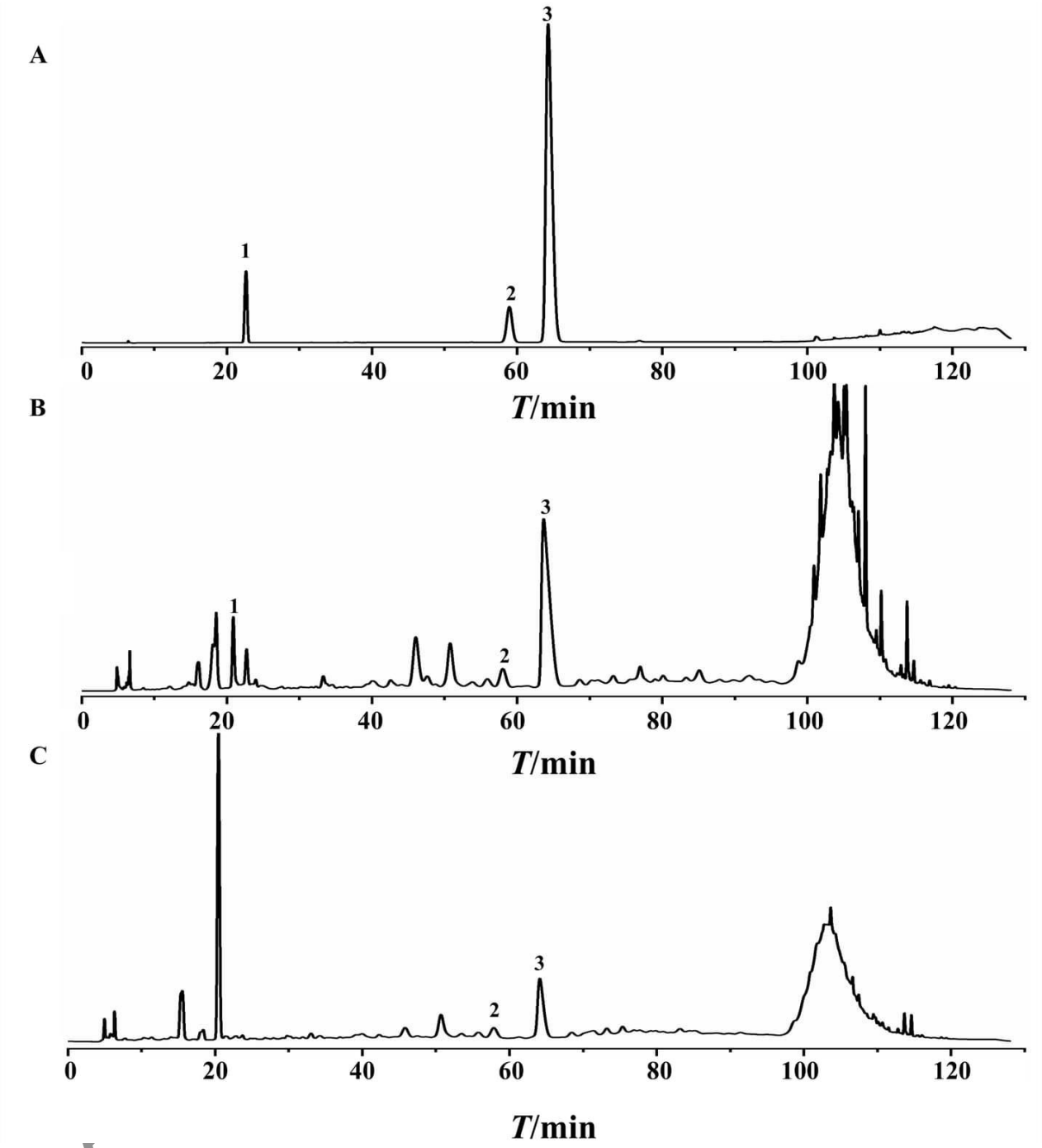


Fig. 1: HPLC chromatograms of mixed reference standards (A), succulent stems (B) and inflorescences (C) of *C. songaricum*. 1. Gallic acid; 2. *p*-Hydroxybenzoic acid; 3. Catechin

These uniform peak characteristics confirmed the credibility of the metabolomic dataset, while the consistent metabolic profiles among the three biological replicates of each tissue further ensured the reliability of inter-tissue metabolic comparisons.

We used metabolomic data from 3 biological replicates of inflorescences and succulent stems of *C. songaricum* to construct a PCA model. The model revealed obvious sample segregation along the two principal components, PC1 (54.6%) and PC2 (20.7%). Together, PC1 and PC2 explained 75.3% of the cumulative variance, indicating that the two principal components captured most of the differential metabolic information between inflorescences and succulent stems.

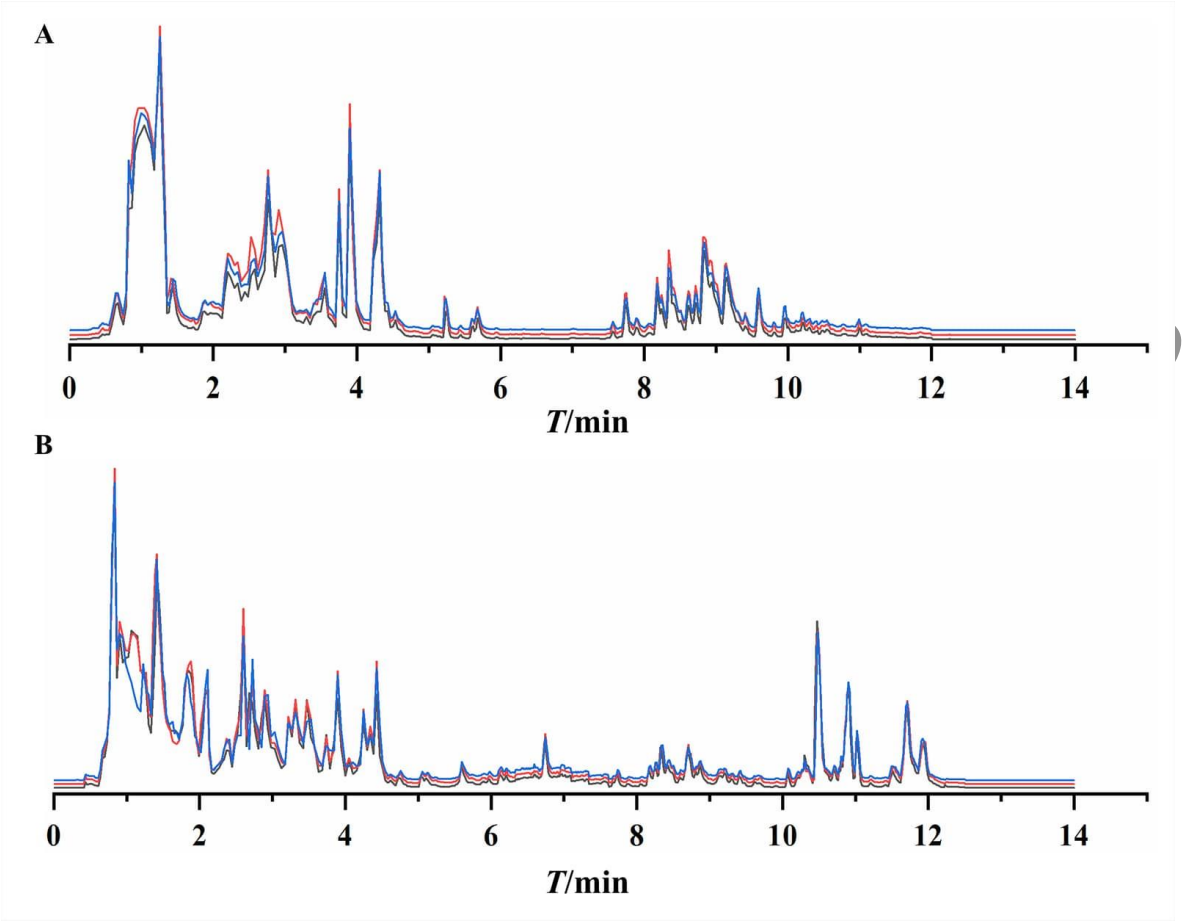


Fig. 2: Overlapped TIC chromatograms of pooled QC samples for widely targeted UPLC–MS/MS metabolomics. (A) Electrospray positive ion mode; (B) Electrospray negative ion mode. Fully overlapped retention times and ion intensity profiles across all repeated QC injections verify stable instrument performance, negligible signal drift and reliable metabolomic dataset for inter-tissue comparison.

Article

As illustrated in the PCA score scatter plot (Fig. 3A), inflorescence and succulent stem specimens formed two fully isolated clusters with minimal intra-group dispersion and excellent experimental repeatability, demonstrating distinct tissue-specific metabolic fingerprints supported by consistent replicate data. Together, these results reflected remarkable metabolic divergence between the two tissue types.

To quantify how individual metabolites drive sample classification, OPLS-DA was then implemented. The corresponding OPLS-DA score plot (Fig. 3B) showed distinct partitioning between inflorescence and succulent stem samples, matching the separation trend observed in PCA and confirming the strong classification capacity of this multivariate statistical model for the two test groups. The established OPLS-DA statistical model yielded key evaluation metrics: R^2_X = 0.805, R^2_Y = 0.995 and Q^2 = 0.973. Among them, R^2_X = 0.805 indicated that the model could explain 80.5% of the total variation of all detected metabolite signals; R^2_Y = 0.995 demonstrated that the model perfectly interpreted the grouping difference between inflorescences and succulent stems; Q^2 = 0.973 far exceeded the threshold of 0.9, proving that the model possessed excellent cross-validation predictive ability and stable classification performance. A total of 200 permutation validation trials (Fig. 3C) were carried out to systematically assess the risk of overfitting in the supervised OPLS-DA model. After random rearrangement of sample grouping labels, the regression fitting curves of R^2 and Q^2 were obtained. The vertical-axis intercept of the Q^2 regression curve fell below zero, which fully complied with the standard for excluding overfitting. This result confirmed that the clear separation between inflorescence and succulent stem samples in the OPLS-DA model reflected real inherent metabolic differences between tissues, rather than random noise or model overfitting due to limited biological replicates (n=3 per group). Using this validated, non-overfitting model, VIP scores were extracted for subsequent differential metabolite screening.

VIP scores were extracted from the fitted model and all compounds possessing VIP > 1 were highlighted in red on the S-plot (Fig. 3D).

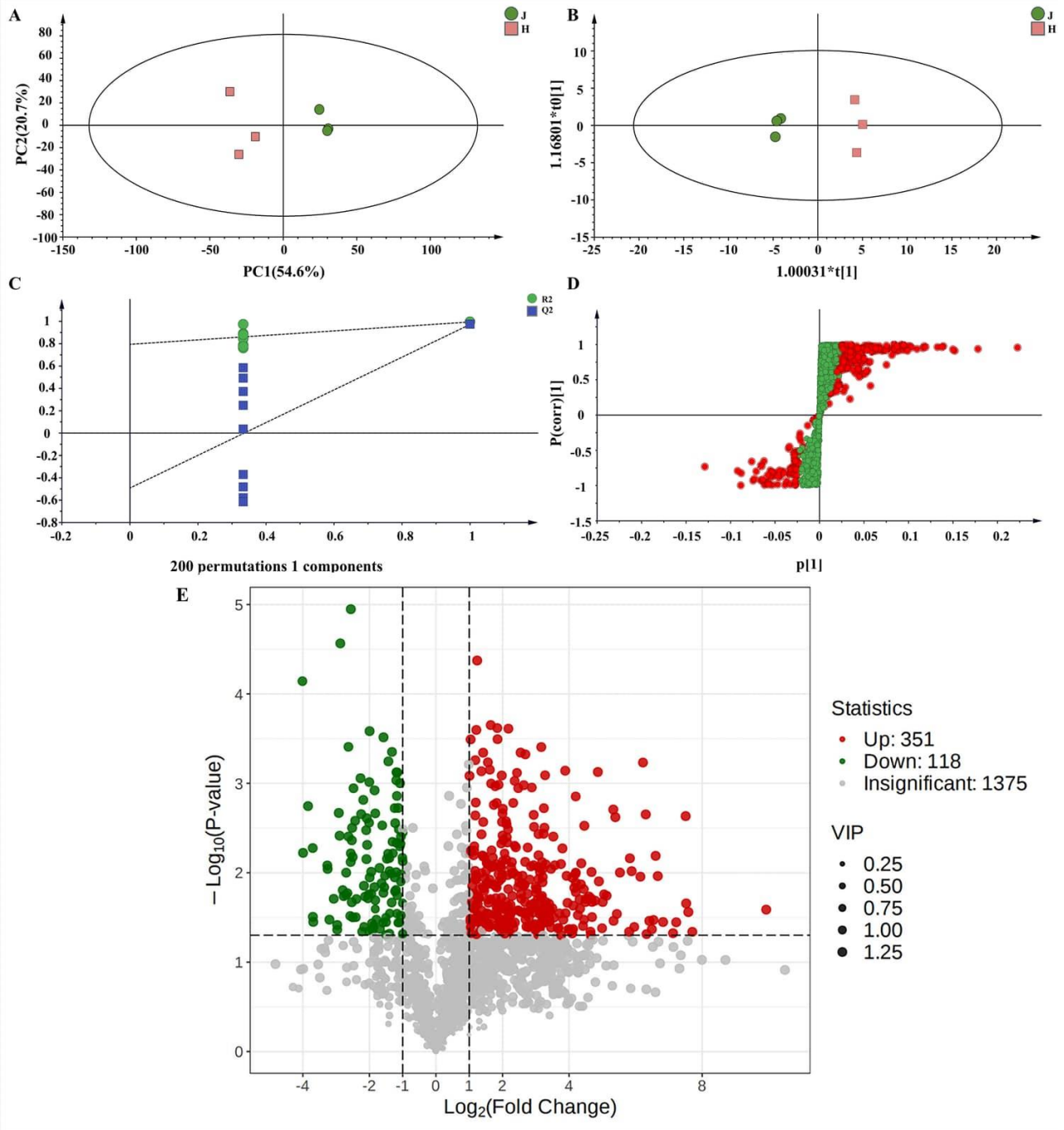


Fig. 3: Multivariate statistical analysis plots of metabolomic data from *C. songaricum* inflorescences (H, red square, n=3) and succulent stems (J, green circle, n=3). (A) PCA score scatter plot, PC1 explained 54.6% total metabolic variation, PC2 explained 20.7%; (B) OPLS-DA classification score plot, evaluation parameters: R^2_X=0.805, R^2_Y=0.995, Q^2=0.973; (C) 200-times permutation test plot for OPLS-DA overfitting assessment; intercept of Q^2<0, no overfitting; (D) S-plot derived from validated OPLS-DA model, red dots: VIP>1, green dots: VIP<1; (E) Volcano plot of differential metabolites, red dots:up-regulated in succulent stems; green dots down-regulated in succulent stems; gray dots: metabolites without significant inter-tissue difference.

To minimize false-positive results from high-throughput multi-metabolite testing, a triple-screening criterion integrating multivariate model parameters, fold change and FDR-adjusted significance was adopted: VIP ≥ 1, FC ≥ 2 or FC ≤ 0.5 and BH-FDR-corrected $p < 0.05$. After strict FDR filtering, 469 compounds originating from 11 metabolite classes were recognized as differential markers, among which 89 were flavonoids, 62 were amino acids and

their conjugates and 59 were phenolic acids. The classifications and counts of remaining metabolites are summarized in table S7.

Global metabolomic profiling revealed that inflorescences and succulent stems shared overlapping metabolite profiles, including flavonoids, amino acid derivatives, lipids, nucleotides and their conjugates, terpenoids, organic acids, tannins, lignans, coumarins and alkaloids. Nevertheless, the quantities of these chemical classes differed markedly between the two plant tissues. Compared with inflorescence samples, succulent stems showed higher abundance of 351 differential metabolites. Most of these metabolites were flavonoids and amino acid derivatives, all of which were marked in red in figure 3E. This finding showed that flavonoids, amino acids and their downstream conjugates accumulated at markedly higher concentrations in stem tissues than in inflorescence parts. In contrast, 118 differential compounds (highlighted in green in Figure 3E) exhibited lower abundance in succulent stems versus inflorescences. These down-regulated metabolites mainly fell into the lignan, coumarin and terpenoid groups, indicating that these chemical species accumulated more abundantly in inflorescences. The full annotation information of metabolites enriched in succulent stems and inflorescences is provided in tables S8 and S9, respectively.

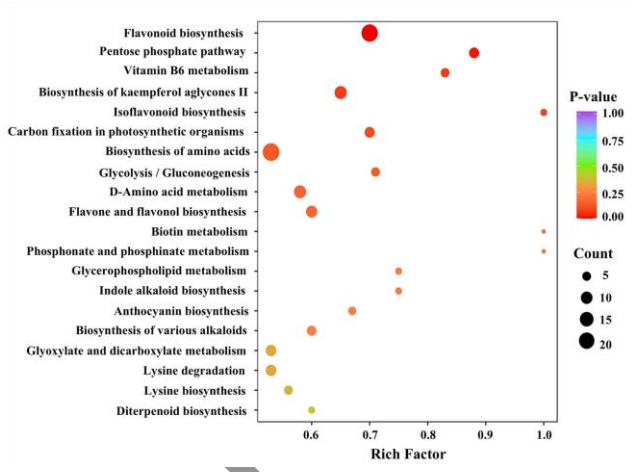


Fig. 4: KEGG pathway enrichment bubble diagram of differential metabolites between *C. songaricum* inflorescences and succulent stems. Horizontal axis = Rich Factor (the ratio of annotated differential metabolite number to total metabolite number in each pathway. Higher value means stronger enrichment); vertical axis = significantly enriched metabolic pathways; bubble color gradient represents BH-FDR corrected *P*-value (red = lower *P*-value, more significant enrichment); bubble size stands for the count of differential metabolites annotated to the corresponding pathway.

KEGG functional enrichment based on the 469 differential metabolites showed that these discriminative compounds were significantly distributed across 20 metabolic cascades (Fig. 4). Among all enriched pathways, flavonoid biosynthesis, biosynthesis of amino acids, pentose phosphate pathway, glycolysis/gluconeogenesis, d-amino acid metabolism and diterpenoid biosynthesis represented the top pathways with prominent enrichment magnitude. Quantitative assays demonstrated that total flavonoids, gallic acid, *p*-hydroxybenzoic acid and catechin were highly enriched in succulent stems. Meanwhile, untargeted metabolomics revealed massive accumulation of amino acids and their derivatives in succulent stems. Accordingly, it was inferred that flavonoid and amino acid biosynthesis are significantly activated in succulent stems. In contrast, quantitative determination showed markedly higher total polysaccharide content in inflorescences; metabolomic data further showed preferential accumulation of lignans, coumarins and terpenoids in inflorescences. Therefore, primary carbon metabolic pathways, including the pentose phosphate pathway and glycolysis/gluconeogenesis, may dominate metabolic processes in inflorescences.

For accurate identification of differential marker metabolites, heatmap visualization was performed for the top 20 differential metabolites exhibiting the most pronounced FC differences (the greatest magnitude of content variation) in inflorescences and succulent stems. Clear tissue-specific accumulation patterns could be observed from the normalised relative abundance profiles. In figure 5A, the 20 down-regulated metabolites in succulent stems exhibited markedly higher signal intensities across all three biological replicates of inflorescence samples. These enriched compounds mainly comprised saccharides, glycosides and terpenoid-related substances such as galactacetophenone, maltotriose, D-galactose, and D-fructose, implying that carbohydrate-derived secondary metabolites are preferentially accumulated in inflorescences. By contrast, the top 20 metabolites up-regulated in succulent stems (Fig. 5B) displayed markedly lower relative abundance in all inflorescence replicates. A large proportion of these compounds belonged to flavonoid oligomers, phenolic acids and tannins, including procyanidin derivatives, ellagic acid-4-*O*-xyloside and galloyl-procyanidin analogues. Consistent with the targeted quantitative results, flavonoid-type polyphenols were found to be dominantly enriched in succulent stem tissues.

Hierarchical clustering further separated inflorescence and succulent stem replicates into independent clades, confirming the reproducible metabolic divergence between the two tissue types. Collectively, the heatmap results visually corroborated the findings from multivariate statistical analysis, showing that inflorescences and succulent stems have distinct metabolite enrichment preferences for carbohydrate-related constituents and polyphenolic compounds, respectively.

Article in Press

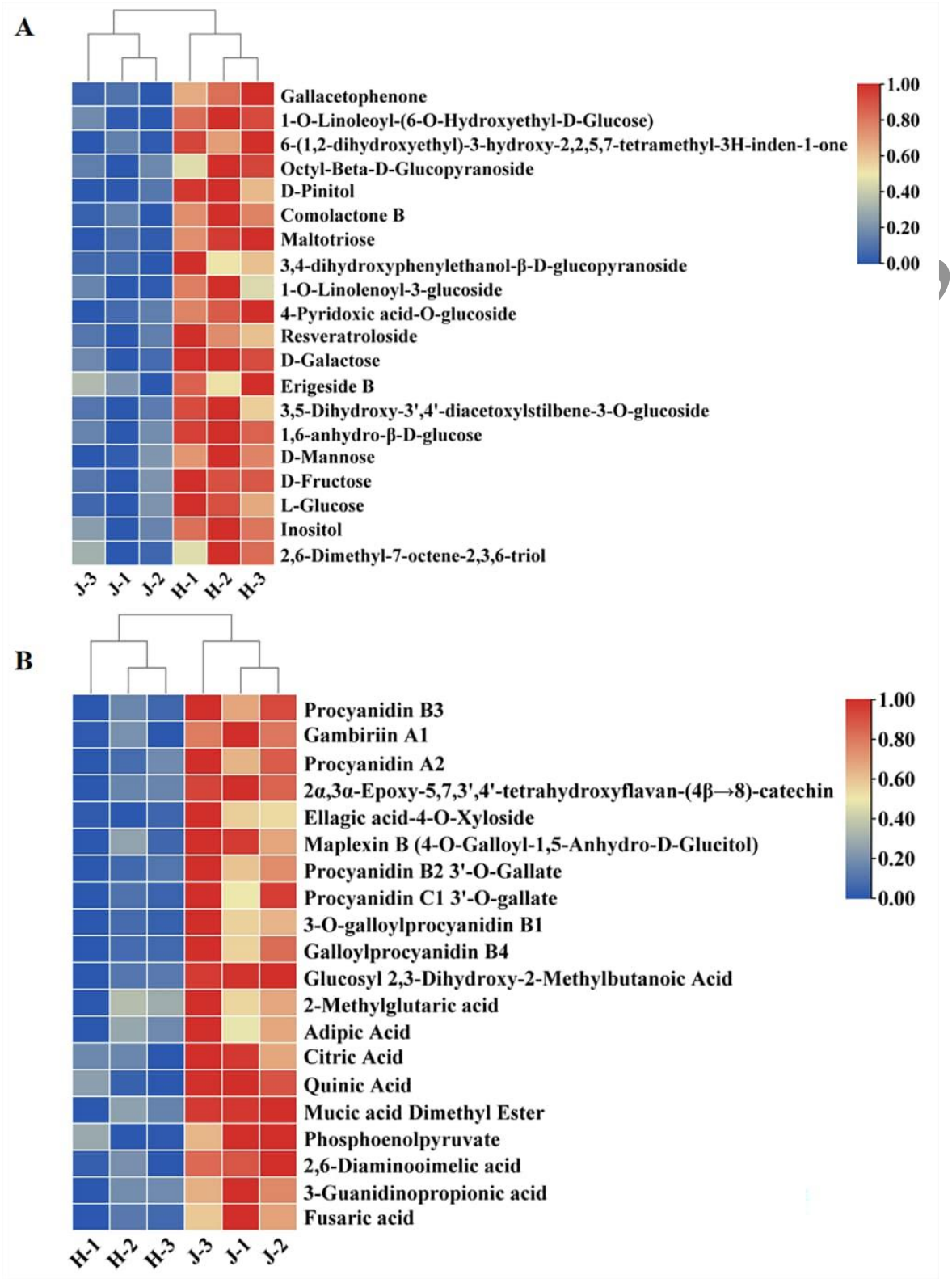


Fig. 5: Heatmap visualization of the top 20 differential metabolites ranked by FC value. (A) Top 20 metabolites significantly enriched in inflorescences (down-regulated in succulent stems compared with inflorescences); (B) Top 20 metabolites significantly enriched in succulent stems (up-regulated in succulent stems compared with inflorescences). The colour gradient from blue to red represents normalized relative metabolite abundance ranging from 0.00 to 1.00. H denotes inflorescences samples, J denotes succulent stems samples.

DISCUSSION

Cynomorium songaricum, known as 'desert ginseng', is a widely used medicinal and edible herb in traditional Chinese, Mongolian and Tibetan medicine, distributed mainly in arid regions of Gansu, Xinjiang and Inner Mongolia (Tu *et al*., 2025). It has long been used in folk herbal medicine to replenish kidney yang and modern studies have validated its pro-fertility, reproductive-protective and anti-benign prostatic hyperplasia activities (Liu *et al*., 2024; Tao *et al*., 2019; Gu *et al*., 2021). It is widely used in proprietary Chinese medicines and health products, such as huqian wan, suoyang gujing wan and guilu bushen wan (Yang *et al*., 2023). However, wild resources are endangered by overharvesting and discarding inflorescences further aggravates resource scarcity (Wang *et al*., 2023). In this study, the chemical compositions of inflorescences and succulent stems were systematically compared using targeted quantitative analysis and widely targeted metabolomics.

This study implemented a three-tier sample screening scheme (50 initial cultivated individuals → 10 quantitative biological replicates → 3 gradient metabolomic replicates) using plant material from a single standardized cultivation base with consistent soil, host, growth cycle and field management, eliminating habitat-driven metabolic bias and ensuring geographic consistency for tissue comparison. From 50 uniform raw plants, 10 morphologically intact, homogeneous individuals were first selected as biological batches (3 technical replicates each) for multi-index quantification; the sufficient sample size yielded robust statistical power for paired t-tests, supported by highly significant inter-tissue differences ($p < 0.001$) and large Cohen's d effect sizes across all five bioactive markers. Given the high cost of widely targeted UPLC-MS/MS, three representative individuals covering low, medium and high gradients of total flavonoids and total polysaccharides were secondarily screened from the ten batches to capture the full chemical variation of the original population. To address the limited metabolomic sample size (n=3), integrated quality control and statistical strategies were used, including continuous pooled QC injection, 200 OPLS-DA permutation tests and triple differential metabolite thresholds (VIP > 1, FC $\geqslant$ 2 or $\leqslant$ 0.5 and BH-FDR-corrected $p < 0.05$). Tight intra-group clustering in PCA plots further validated high reproducibility and reliability of the metabolomic dataset.

The results showed that succulent stems were richer in total flavonoids, gallic acid, *p*-hydroxybenzoic acid and catechin. The KEGG enrichment results further elucidated the metabolic basis underlying tissue-specific chemical profiles and can be cross-validated with the targeted quantitative datasets from UV–Vis and HPLC. The strong enrichment of flavonoid-related biosynthetic pathways in succulent stems is consistent with its higher total flavonoids, catechin and *p*-hydroxybenzoic acid, as well as the exclusive occurrence of gallic acid within this medicinal tissue. Metabolites produced by these pathways are major contributors to the well-documented antioxidant, anti-fatigue and neuroprotective activities of *C. songaricum* (Ma *et al*., 2023; Yu *et al*., 2008; Wang *et al*., 2025; Lyu *et al*., 2023). These pharmacological properties are closely linked to the traditional kidney-yang-tonifying use of *C. songaricum*. Enrichment of amino-acid biosynthesis in succulent stems further complements its bioactive metabolite reservoir and may support immunomodulatory effects (Wang *et al*., 2022).

For inflorescences, significant enrichment of diterpenoid biosynthesis and abundant accumulation of phenylpropanoid-derived lignans and coumarins suggest that inflorescences exhibited a distinct secondary-metabolite-synthesis profile compared with succulent stems. Lignans, coumarins and terpenoids exert antioxidant, hepatoprotective, neuroprotective and immunomodulatory bioactivities (Zhang *et al*., 2022a; Chen and Ko, 2013; Chen *et al*., 2014), implying that inflorescences may exert bioactivity through metabolite classes partially distinct from succulent stems. Differences in the pentose phosphate pathway and glycolysis/gluconeogenesis, in turn, provide a metabolic explanation for the higher total polysaccharide content determined in inflorescences. Polysaccharides from *C. songaricum* are known for their immunomodulatory, osteogenic and hypoglycaemic effects (Lv *et al*., 2023; Hu *et al*., 2022; Shi *et al*., 2021). Taken together, pathway-level evidence combined with the quantitative chemical data supports the core hypothesis: discarded inflorescences are not metabolically inert waste but harbor tissue-specific bioactive constituents assembled by functional biosynthetic cascades.

Heatmap visualization of the top 20 differential metabolites with the largest FC differences further consolidated the above conclusions. Procyanidin oligomers, ellagic acid-4-*O*-xyloside and tannins were highly enriched in succulent stems. Together with HPLC-detected catechin, gallic acid and *p*-hydroxybenzoic acid, these polyphenols represent key candidate bioactive compounds underlying the pharmacological actions of succulent stems, consistent with the previously reported antioxidant, anti-fatigue and reproductive-protective effects of *C. songaricum* polyphenols (Yu *et al*., 2008; Wang *et al*., 2025; Lyu *et al*., 2023). In inflorescences, results indicating abundant soluble saccharides agreed with colorimetric measurements of higher total polysaccharides, alongside preferential accumulation of lignans, coumarins

Article in Press

and terpenoids. Although these inflorescence-enriched metabolites have documented bioactivities, their contribution to kidney-yang-tonifying efficacy remains unproven. Accordingly, chemical evidence supports resource-development potential for inflorescences but cannot confirm *in-vivo* pharmacological performance. Given the complete absence of gallic acid and markedly reduced flavonoid and catechin levels in inflorescences, they cannot serve as a direct substitute for succulent stems in kidney-yang-tonifying applications. Instead, inflorescences should be developed as complementary healthcare raw materials, enabling differentiated and rational utilization of the two *C. songaricum* tissues.

The remarkable tissue-specific metabolic divergence observed in the present study can be partially interpreted from the perspective of plant physiological adaptation. *Cynomorium songaricum* is an obligate root-parasite growing in desert saline-alkali habitats (Zhang *et al*., 2022b). The succulent stems act as the underground vegetative storage organ connected to host haustoria, whereas inflorescences are the aerial reproductive organs responsible for flowering and seed formation. Distinct physiological roles of these two organs redirect carbon partitioning and secondary-metabolite biosynthetic flux, finally generating divergent chemical fingerprints (Sun *et al*., 2021). Underground succulent stems are continuously exposed to soil salinity, drought stress and soil-borne microorganisms; therefore, they biosynthesize large quantities of flavonoids, catechin, gallic acid and tannins as defensive and antioxidant metabolites to resist harsh subterranean environments and mediate host–parasite interactions (Sun *et al*., 2021). By contrast, inflorescences prioritize carbon allocation toward polysaccharide production to supply energy and carbon skeletons for floral growth and seed development. Lignans, coumarins and terpenoids accumulated in inflorescences may protect reproductive tissues against above-ground herbivory, ultraviolet radiation and pathogenic infection during anthesis. Such metabolic tissue specialization represents an adaptive physiological strategy for this desert-parasitic medicinal plant.

Tissue-specific metabolic differentiation between reproductive and vegetative organs is a widespread phenomenon among medicinal root parasitic plants. For example, *Cistanche deserticola*, another desert-adapted obligate root parasite within Orobanchaceae, exhibits clear organ-biased distribution of phenylethanoid glycosides: stem tissues accumulate high levels of echinacoside and verbascoside, whereas floral parts contain relatively lower phenylethanoid glycosides but are rich in polysaccharides and terpenoid constituents (Sun *et al*., 2021), consistent with the observation in *C. songaricum* that vegetative succulent stems accumulate signature phenolic markers while reproductive inflorescences favour polysaccharide- and terpenoid-related metabolism. Nevertheless, one distinct feature of *C. songaricum* revealed in this work is the complete absence of gallic acid in inflorescences; such strict organ-restricted accumulation of a core quality marker phenolic compound has rarely been documented in other desert-parasitic medicinal plants.

For many endangered or nationally protected medicinal herbs, harvesting only pharmacopoeia-specified medicinal parts generates large volumes of discarded by-products, creating resource-waste dilemmas similar to those seen with *C. songaricum*. For instance, *Glycyrrhiza uralensis* is mainly used medicinally for its rhizomes and roots, while overground aerial parts are routinely discarded; metabolomic investigations have shown that aerial tissues contain abundant phenolic acids and flavonoids, providing chemical evidence for their potential development as complementary resources (Jiang *et al*., 2021). Similarly, *Panax ginseng* fibrous roots and leaves are processing by-products, which contain characteristic ginsenosides with distinct component profiles compared with the main taproots (Kang and Kim, 2016). For these endangered species, researchers commonly advocate multi-tissue chemical profiling before exploiting by-products, rather than treating waste tissues as direct substitutes for official medicinal materials. This principle is closely aligned with conclusions drawn for *C. songaricum*: inflorescences contain unique bio-metabolites but cannot replace succulent stems for established therapeutic purposes and pharmacological validation is mandatory prior to practical application. Collectively, the lessons from *C. songaricum* extend to other endangered medicinal plants: when wild populations are threatened by overharvesting, multi-platform chemical comparison of discarded plant fractions is a feasible first step to explore by-product potential, relieve exploitation pressure on official medicinal organs and advance circular conservation (Jiang *et al*., 2021). Importantly, chemical profiling alone cannot prove pharmacological efficacy, which remains a universal bottleneck for by-product resource development across parasitic and endangered medicinal herbs.

Compared with existing phytochemical and metabolomic investigations of *C. songaricum*, this study makes the following key advances: a multi-index quantitative system that simultaneously quantifies total polysaccharides, total flavonoids and three phenolic markers was constructed and it was first verified using HPLC that gallic acid only accumulates in succulent stems to overcome the drawback of conventional single or dual marker testing. A widely targeted UPLC-MS/MS metabolomic comparison of the two tissues was pioneered, with 469 differential metabolites belonging to 11 classes annotated and tissue-specific metabolite enrichment that cannot be detected via

Article in Press

single-marker quantification revealed. Finally, the combined dataset of macro-component detection, HPLC analysis and metabolomics forms an integrated chemical evidence system that proves the resource-exploration potential of inflorescences, resolves industrial biomass waste problems, provides theoretical support for reducing wild-stem exploitation and conserving this endangered plant and delivers stronger practical significance than prior stem-only chemical analyses.

The present study has several limitations. First, all 469 differential metabolites screened by UPLC-MS/MS were annotated only by spectral matching against the MWDB database, without using authentic chemical standards for confirmation; this high-throughput, database-dependent annotation cannot completely rule out isomeric compounds with similar fragmentation patterns. Thus, future work should validate the structures of key tissue-specific differential metabolites (e.g., representative lignans, coumarins and flavonoid aglycones) using isolated pure compounds and reference standards. Second, only chemical quantification and metabolomic profiling were performed and no pharmacological assays were conducted on *C. songaricum* inflorescences. Despite reported bioactivities of some inflorescence-enriched metabolites from prior compound-level studies, direct experimental evidence supporting the bioactivities of inflorescence extracts, particularly its kidney-yang-tonifying effects, is lacking and the association between metabolite content and *in-vivo* biological function remains unproven. Moreover, a definite causal relationship cannot be established between differential metabolites and the classical kidney-yang-tonifying action of *C. songaricum*, as this holistic pharmacological effect is derived from multi-component synergism and the metabolite–effect relationship has not been fully elucidated even for the official succulent stems. Whether inflorescence-accumulated lignans, coumarins, terpenoids and polysaccharides participate in kidney-yang-tonifying activity still requires investigation; therefore, no definitive conclusions can be drawn about the medicinal value of inflorescences for this indication.

Future research priorities are explicitly listed: (1) Safety and toxicity assessment of inflorescence raw materials: Safety evaluation should cover not only general toxicological endpoints but also potential metabolic activation and drug-metabolizing enzyme- and transporter-related risks of herbal extracts, as highlighted in a previous herbal toxicology review (Wu *et al*., 2024b). (2) Cell-based and *in-vivo* pharmacological comparison between inflorescence and succulent stem extracts, focusing on pharmacodynamic indicators related to kidney-yang-tonifying activity: *In-vivo* pharmacological evaluation combined with histopathological and biochemical biomarker detection is an effective strategy to verify crude extract efficacy, as reported in previous herbal medicinal studies (Lou *et al*., 2024). (3) Bioactivity-guided separation and identification of key active constituents from inflorescences (Chen *et al*., 2019): Effect-directed fractionation represents a mature workflow to pinpoint bioactive compounds from complex herbal matrices, which can be adopted to screen and isolate tissue-specific bioactive metabolites of *C. songaricum* (Zeng *et al*., 2018). For plant polysaccharides, a complete analytical pipeline combining column-based purification, monosaccharide composition analysis, spectroscopic structural elucidation and in vitro cell-based functional verification is strongly recommended for characterizing inflorescence-derived polysaccharide fractions (Xiao *et al*., 2024). (4) After obtaining purified bioactive monomers via bioactivity-guided fractionation, further in-depth pharmacokinetic investigations including plasma concentration–time profile, tissue distribution, absolute oral bioavailability, as well as sex-dependent metabolic differences should be implemented to provide critical preclinical data for drug development (Shang *et al*., 2024).

From a practical processing perspective, discarded inflorescences are currently removed during primary raw-material sorting of *C. songaricum* and these by-products can be collected on site without additional harvesting costs. The preliminary processing workflow may include manual impurity removal, shade or low-temperature (40–45 °C) hot-air drying, pulverization and sieving. For further utilization, solvent-based extraction (ethanol-water or hot-water reflux) can be used to enrich polysaccharide-, lignan-, coumarin- and terpenoid-enriched fractions from inflorescence powder. Given its high polysaccharide abundance and unique secondary-metabolite profile, inflorescence material shows potential as a complementary feedstock for antioxidant-focused healthcare products, plant-derived functional additives, or raw material for further bioactivity screening, rather than a direct substitute for pharmacopoeia-defined medicinal succulent stems.

Nevertheless, several economic and industrial barriers remain unresolved at present. First, inflorescence material lacks established QC standards; no unified specifications exist for harvesting time, drying parameters, or component acceptance criteria. Second, target bioactive components in inflorescences have not been pharmacologically validated, so dosage–effect relationships and safety profiles remain unknown, which blocks regulatory approval for medicinal use. Third, the separation and purification cost for low-abundance lignans, coumarins and terpenoids is relatively high. Therefore, large-scale industrial exploitation cannot be achieved based solely on the current chemical evidence. At this stage, its value is reflected more clearly in circular resource reuse: making full use of

Article in Press

otherwise discarded processing by-products to ease collection pressure on wild succulent stem resources partially. Further pharmacological verification, quality-standard formulation and cost-optimization of separation processes are prerequisites before real industrial deployment.

Inflorescence reuse improves resource efficiency only for already harvested individuals. It cannot offset the damage caused by overharvesting whole wild plants. Long-term sustainability for *C. songaricum* still depends on expanded, standardized artificial cultivation, strict wild-harvest quotas and habitat conservation. The by-product development strategy described in this paper is a complementary measure rather than a standalone solution for endangered plant conservation.

Harvesting season, plant age and host-plant identity are major sources of metabolic variation in root-parasitic medicinal plants such as *C. songaricum.* In the current investigation, these factors were strictly standardized to compare intrinsic chemical differences between inflorescences and succulent stem tissues. Under practical production and wild-collection scenarios, variations in growing season, maturity status, or host species may alter the absolute contents of flavonoids, polysaccharides, phenolic acids, lignans and terpenoids in both tissue types, which may further change the relative quantitative ratios between inflorescences and succulent stems. Therefore, the tissue-specific accumulation patterns observed in this study were obtained under controlled cultivation conditions. Further work is required to assess how seasonal fluctuation, plant age and host-plant types reshape metabolomic profiles of inflorescences and succulent stems, which will support future formulation of practical QC specifications for inflorescence by-products.

CONCLUSION

This study systematically revealed the compositional differences between inflorescences and succulent stems of *C. songaricum* using targeted quantification and widely targeted metabolomics. Succulent stems were enriched in total flavonoids, gallic acid, *p*-hydroxybenzoic acid and catechin, while inflorescences contained higher total polysaccharides and showed higher abundances of lignans, coumarins and terpenoids. These detected chemical constituents have been reported to exhibit bioactivities in separate compound-level studies. The observations indicate only possible resource-development value for inflorescences at the compositional level, without confirming any in vivo pharmacological effects, particularly kidney-yang-tonifying efficacy. This study did not establish a metabolite–effect causal relationship for kidney-yang-tonifying function. Although this study did not evaluate pharmacological activities, the presence of multiple bioactive metabolites and the well-documented kidney-yang-tonifying efficacy of *C. songaricum* support further pharmacological investigation of inflorescences. Future research should prioritize pharmacological validation, including kidney-yang-tonifying-related pharmacodynamic evaluation, bioactivity-guided compound isolation, safety assessment and product development. Direct pharmacological evidence is required before considering any medicinal applications of inflorescence by-products.

A hypothesis was constructed prior to experimentation and systematically validated using combined spectrophotometry, HPLC and broad-spectrum metabolomics. The results were consistent with predictions that discarded inflorescences contain abundant tissue-specific bio-related metabolites rather than being chemically inert waste. Nevertheless, the hypothesis addresses only chemical composition differences and resource potential and does not claim pharmacological efficacy of inflorescences. Therefore, further pharmacological assays targeting kidney-yang-tonifying activity are required to extend and supplement the present hypothesis. Collectively, this work transcends the single-tissue, single-index research mode of existing studies on *C. songaricum*, establishes a systematic chemical comparison system for inflorescences and succulent stems and delivers original comprehensive metabolomic data of inflorescences; these findings bridge the existing research gap on the chemical basis of waste inflorescences and lay a more complete theoretical foundation for the circular utilization of this protected medicinal resource.

Acknowledgements

The authors would like to thank the Key Laboratory of Hexi Corridor Resources Utilization, Gansu Province, China, the Science and Technology Department of Gansu Province, China and Hexi University for providing support in this study. The authors express heartfelt gratitude to the editors and reviewers for their suggestions. Meanwhile, the authors acknowledge the use of the AI tool Doubao in the preparation of this manuscript. This artificial intelligence tool was mainly used for assisting manuscript writing, text polishing and language editing during the research paper compilation process. All authors take full responsibility for the originality, accuracy and integrity of all content in the final revised manuscript.

Authors' contributions

Qin Wang and Yuxia Song: Conceptualization; Lin Yang and Jiaqi Hu: Data curation; Congying Li: Formal analysis, methodology and writing – original draft; Yumei Wang: Supervision; Zhongjie Bai: Visualization; Congying Li and Yumei Wang: Writing – review and editing.

Article in Press

Funding
The study was funded by Key Laboratory of Hexi Corridor Resources Utilization, Gansu Province, China (No. XZ2307), the Natural Science Foundation of Gansu Province, China (No. 24JRRG020 and No. 23JRRG0036), the Science and Technology Plan Project of Zhangye City, Gansu Province, China (No. ZY2025BJ43), the Doctoral Research Startup Fund of Hexi University (No. KYQD2024005) and President's Fund Team Project of Hexi University (No. CXTD2024007).

Data availability statement
The datasets generated during and/or analysed during the current study are available from the corresponding author on reasonable request.

Ethical approval
Not applicable. The *Cynomorium songaricum* materials used in this work were purchased from artificial cultivation bases and no wild plant collection was conducted. This study did not involve human participants or animal experiments. All plant materials were legally acquired and no protected wild species were sampled.

Conflict of interest
The authors declare no conflict of interest.

REFERENCES

Aruna, Tong L, Dai W, Shao W, Hai Y. and Jirimubata (2025). Key components and mechanism analysis of mongolian medicine *Cynomorium songaricum* for chronic atrophic gastritis based on "Component-Flavor-Efficacy" Correlation. *J. Inner Mongol. Med. Univ.,* **47**(6): 568-573.

Chen J and Ko KM (2013). Ursolic-acid-enriched herba *Cynomorii* extract protects against oxidant injury in H9c2 cells and rat myocardium by increasing mitochondrial ATP generation capacity and enhancing cellular glutathione redox cycling, possibly through mitochondrial uncoupling. *Evid. based Complement. Altern. Med.,* **2013**: 1-14.

Chen J, Wong HS, Leung HY, Leong PK, Chan WM, Chen N and Ko KM (2014). An ursolic acid-enriched extract of *Cynomorium songaricum* protects against carbon tetrachloride hepatotoxicity and gentamicin nephrotoxicity in rats possibly through a mitochondrial pathway: A comparison with ursolic acid. *J. Funct. Foods,* **7**(2014): 330-341.

Chen W, Zhang H, Wang J and Hu X (2019). A New Triterpenoid from the Bulbs of *Lilium speciosum* var. *gloriosoides*. *Chem. Nat. Compd.,* **55**(2): 289-291.

Feng H, Ye W, Wang W, Song M, Hou J and Chang Y (2026). Comparative analysis of degumming effects on the structural profiles and physicochemical properties of *Idesia polycarpa* phospholipids. *Food Chem.,* **502**(2026): 147682.

Gu J, Li Z, Qi Y and Cao Y (2021). The effect of *Cynomorium* on the semen quality and sex hormone level in the oligospermia rat model. *Contemp. Med.,* **27**(13): 14-16.

Guo Y, Gu Z, Qi M, Lv X, Zhang R, Xv A and Ge B (2022). Multi-index comprehensive quality evaluation of *Cynomorium songaricum* from different producing areas based on projection pursuit model. *Chin. Wild Plant Resour.*, **41**(8): 14-21.

Hu J, Tan R, Yuan Z, Yang P, Zhang C, Zhang B and Shen Y (2022). *Cynomorium songaricum* polysaccharide promotes osteogenic differentiation of MC3T3-E1 cells by activating PI3K/Akt/GSK3β/β-catenin signaling pathway. *J. Pract. Med.,* **38**(22): 2774-2779.

Jiang L, Akram W, Luo B, Hu S, Faruque MO, Ahmad S, Yasin NA, Khan WU, Ahmad A, Shikov AN, Chen J and Hu X (2021). Metabolomic and pharmacologic insights of aerial and underground parts of *Glycyrrhiza uralensis* Fisch. ex DC. for maximum utilization of medicinal resources. *Front. Pharmacol.,* **12**:658670.

Kang O-J and Kim J-S (2016). Comparison of ginsenoside contents in different parts of Korean ginseng (*Panax ginseng* C.A. Meyer). *Prev. Nutr. Food Sci.,* **21**(4): 389-392.

Lan Z, Wang Y, Xie R and Xu L (2025). Research progress of historical development, chemical composition and pharmacological effects on the processing of *Cynomorium songaricum*. *China J. Tradit. Chin. Med. Pharm.*, **40**(6): 2980-2986.

Liu L, Liu C, Sun T, Li G and Xu G (2024). Effect of *Cynomorium songaricum* water extract on testicular injury induced by cyclophosphamide in mice. *J. Huaibei Norm. Univ. (Nat. Sci.)*, **45**(1): 56-61.

Liu X, Liu X, Ma H, Wang X, Chen Z, Luo W And Yang F (2025). Widespread targeted metabolomics study of different organs in Codonopsis tangshen (Wendang). *Chin. Tradit. Pat. Med.*, **47**(6): 2072-2077.

Lou Y, Zou X, Pan Z, Huang Z, Zheng S, Zheng X, Yang X, Bao M, Zhang Y, Gu J and Zhang Y (2024). The mechanism of action of *Botrychium (Thunb.)* Sw. for prevention of idiopathic pulmonary fibrosis based on ^{1}H-NMR-based metabolomics. *J. Pharm. Pharmacol.,* **76**: 1018-1027.

Lv T, Chen J, He Z, Chen W, Zong Y and Du R (2023). Studies of the immunomodulatory activity of polysaccharides from the stem of *Cynomorium songaricum* based on intestinal microbial analysis. *Molecules,* **29**:143.

Lyu X, Gu Z, Qi M, Guo Y, Mao X and Ge B (2023). Effects of *Cynomorium songaricum* flavonoids on ROS content and expression of NADPH oxidase and NLRP3 in the hippocampus of alzheimer disease rats. *Chin. J. Inf. Tradit. Chin. Med.*, **30**(4): 82-87.

Article in Press

Ma L and Chen G (2008). The difference of the active compoents from the different segments of the succulent stem of *Cynomorium songaricum* Rupr. *Lishizhen Med. Mater. Med. Res.*, **19**(12): 2913-2914.

Ma Y, Wei C, Xu X, Lu X, Wang Y and Duan X (2023). Study on p-hydroxybenzoic acid on rheumatoid arthritis via inhibiting NF-κB/caspase-1 signaling pathway. *Chin. J. Mod. Appl. Pharm.,* **40**(18): 2519-2525.

Meng J, Ding C, Peng S, Liu Y, Yan J and Cui P (2023). Simultaneous determination of seven different components in *Cynomorium songaricum* Rupr. by QAMS. *Acta. Pharm. Sin.*, **58**(9): 2763−2770.

National Pharmacopoeia Committee. *Pharmacopoeia of the People's Republic of China*. Beijing: China Medical Science Press, 2025.

Peng J, Ge C, Shang K, Liu S and Jiang Y (2024). Comprehensive profiling of the chemical constituents in Dayuanyin decoction using UPLC-QTOF-MS combined with molecular networking. *Pharm. Biol.,* **62**(1): 480-498.

Qin C, Zhang S, Tian M, Wang Y, Xu G, Guo C and Li Y (2025). Processing history, chemical constituents and pharmacological effects of *Cynomorium songaricum*: A review. *World. Chin. Med.*, **20**(16): 2958-2970.

Shang K, Ge C, Zhang Y, Xiao J, Liu S and Jiang Y (2024). An evaluation of sex-specific pharmacokinetics and bioavailability of kokusaginine: An *in-vitro* and *in-vivo* investigation. *Pharmaceuticals,* **17**:1053.

Shi S, Li K, Peng J, Li J, Luo L, Liu M, Chen Y, Xiang Z, Xiong P, Liu L and Cai W (2022). Chemical characterization of extracts of leaves of *Kadsua coccinea* (Lem.) A.C. Sm. by UHPLC-Q-Exactive Orbitrap Mass spectrometry and assessment of their antioxidant and anti-inflammatory activities. *Biomed. Pharmacother.,* **149**(2022):112828.

Shi ZQ, Wang LY, Zheng JY, Xin GZ and Chen L (2021). Lipidomics characterization of the mechanism of *Cynomorium songaricum* polysaccharide on treating type 2 diabetes. *J. Chromatogr. B*, **1176** (2021):122737.

Song Y, Guan J, Wang Q, Li C and Li S (2025). Comparative study on quality of fresh-cut pieces and traditional decoction pieces of *Cynomorium songaricum* Rupr. *Mod. Chin. Med.*, **27**(6): 1106-1113.

Sun X, Zheng Y, Tian L, Miao Y, Zeng T, Jiang Y, Pei J, Ahmad B and Huang L (2021). Metabolome profiling and molecular docking analysis revealed the metabolic differences and potential pharmacological mechanisms of the inflorescence and succulent stem of *Cistanche deserticola*. *RSC Adv.,* **11**: 27226-27245.

Tao R, Miao L, Yu X, Orgah JO, Barnabas O, Chang Y, Liu E, Fan G and Gao X (2019). *Cynomorium songaricum* Rupr. demonstrates phytoestrogenic or phytoandrogenic like activities that attenuates benign prostatic hyperplasia via regulating steroid 5-α-reductase. *J. Ethnopharmacol.*, **235**(2019): 65-74.

Tu G, Xi S, Guo X, Gong H, Chen F, Zhu T, Liu L and Jin L (2025). Analysis on geographical distribution pattern simulation and influencing factors of potential suitable areas for *Cynomorium songaricum* Rupr. *Chin. J. Inf. Tradit. Chin. Med.*, **32**(9): 1-6.

Wang J, Wang K, Cheng R, Zhang K and Pei J (2022). Research progress of amino acids in *Cynomorium songaricum*. *Biotic Resources,* 44(6): 517-524.

Wang J, Wang W, Li M, Zhou Y and Li Y (2023). Determination and analysis of nutritional components in *Cynomorium songaricum* parasitic on two species of Nitraria. *J. Gansu Agric. Univ.*, **58**(2): 130-136.

Wang L, Miao J, Wang Y-M, Li C-Y and Huang D-D (2024). Correlation of four active ingredients with ecological factors in *Cynomorium songaricum* from different regions of Hexi, Gansu. *J. Hexi Univ,* **40**(5): 1-8.

Wang Y, Wang Y, Li N and Li C (2025). Correlation between total flavonoids and total polyphenols content with antioxidant activities of different extracts of *Cynomorium songaricum*. *Nat. Prod. Res. Dev.*, **37**(9): 1638-1644.

Wu Q, Zhao D, Leng Y, Chen C, Xiao K, Wu Z and Chen F (2024a). Identification of the Hypoglycemic Active Components of *Lonicera japonica* Thunb. and *Lonicera hypoglauca* Miq. by UPLC-Q-TOF-MS. *Molecules,* **29**: 4848.

Wu Z, Shangguan D, Huang Q and Wang Y-K (2024b). Drug metabolism and transport mediated the hepatotoxicity of *Pleuropterus multiflorus* root: A review. *Drug Metab. Rev.,* **56**(4): 349-358.

Xiao L, Hou J, Chen P, Tan X, Qin X, Nie J, Zhu H and Zhong S (2024). Isolation, characterization and activity of the polysaccharides in *Bulbophyllum kwangtumgense* Schltr. *Int. J. Biol. Macromol.,* **283**(2024): 137382.

Yang H, Gu Z, Guo Y, Mao X, Qi M and Ge B (2023). Research progress in the development and application of *Cynomorium songaricum* related preparations and health products. *Chin. Wild Plant Resour.*, **42**(5): 83-88.

Yu F, Feng S, Xie M and Lian X (2008). Anti fatigue effect of *Cynomorium songaricum* flavone on old rats. *Chin J. Rehabil. Theory Pract.,* **14**(12): 1141-1142.

Zeng G, Wu Z, Cao W, Wang Y, Deng X and Zhou Y (2018). Identification of anti-nociceptive constituents from the pollen of *Typha angustifolia* L. using effect-directed fractionation. *Nat. Prod. Res.,* **34**: 1041-1045.

Zhang B, Yang SL, Li X, Zhang QR, Tian MY, Wang XL and Wang SJ (2022a). Structures and neuroprotective activities of triterpenoids from *Cynomorium coccineum subsp. songaricum* (Rupr.) J. Leonard. *Phytochemistry,* **198**(2022): 113155.

Zhang H, Ji X, Cui J, Wang J, Wang M and Qin X (2022b). Community structure and functional characteristics of endophytic bacteria in root-parasitic plant *Cynomorium songaricum* and its host *Nitraria tangutorum*. *J. Shanxi*

Article in Press

Univ. (Nat. Sci. Ed.), **45**(6): 1640-1647.

Zhang Q, Li B, Wang Z, Feng X, Ji J and Chen G (2023). Analysis of genes related to the biosynthesis pathway of catechin in *Cynomorium songaricum*. *Forest Ecol Sci,* **38**(2): 209-217.

Zhang Q, Rena K, Wang X, Wang X and Wang X (2007). Studies on the chemical constituents of flavonids in the inflorescences of *Cynomorium songaricum* Rupr. *J. Xinjiang Med. Univ.*, **30**(5): 466-468.

Zhang R, Gu Z, Lyu X, Mao X, Guo Y, Qi M and Ge B (2021). Construction of multi-index evaluation system and optimization of weight allocation method for the quality of *Cynomorii herba*. *Chin. J. Inf. Tradit. Chin. Med.*, **28**(12):74-81.

Zhang Y, Yang X and Wang Q (2025). Optimization of extraction technology of catechin and phloridzin in *Cynomorii Herba* by Box-Behnken response surface methodology. *J. Tradit. Chin. Vet. Med.*, **44**(6):63-70.

Article in Press